Ionization of excited hydrogen atoms interacting with a metal surface under the influence of an external electric field

P. Kürpick* and U. Thumm
J.R. Macdonald Laboratory, Department of Physics, Kansas State University, Manhattan, Kansas 66506-2601

U. Wille
Bereich Theoretische Physik, Hahn-Meitner-Institut Berlin, Glienicker Strasse 100, D-14109 Berlin, Germany
(Received 2 October 1997)

Ionization probabilities for highly excited hydrogen atoms interacting with a metal surface are calculated within the time-dependent close-coupling approach. In order to simulate current experiments, the effect of a uniform external electric field is taken into account. Adiabatic resonance states determined in the fixed-atom approximation are used as basis states in the time-dependent calculations. The velocity-dependent dynamic couplings acting between the resonance states are found to influence the total ion production for low-velocity Rydberg atoms. [S1050-2947(98)00903-2]

PACS number(s): 79.20.Rf, 32.80.Rm

I. INTRODUCTION

The ionization of excited atoms represents a simple and transparent example for the electronic processes that can occur when slowly moving atoms or ions interact with metal surfaces [1–4]. While ion neutralization in front of metal surfaces in general involves multiple one-electron processes [5,6] as well as (Auger-like) two-electron processes [7], the ionization of excited atoms may be viewed as (direct) resonant one-electron transfer into empty conduction-band states (''resonance ionization''). A major incentive to study resonance ionization of excited atoms derives from the expectation that, by measuring the atom-surface distances at which the ionizing transitions take place (''ionization distances''), one might be able to obtain information on the electronic potential at large distances. It has been suggested [3] that ionization distances of Rydberg atoms may be determined by measuring the ion yield as a function of an applied external field, which counteracts the attractive image force exerted by the surface on the ions and which removes them from the interaction region. The accurate determination of ionization distances from the measured ion signals requires a quantitative theoretical analysis in which the time evolution of the ionization process is carefully evaluated, taking into account the effect of the electronic surface potential as well as that of the applied external field.

While initial experiments using the technique of Ref. [3] remained inconclusive [8], promising new experiments are currently being undertaken [9] in which an atom in a high-n Rydberg state slowly approaches a metal surface (with a perpendicular velocity of $\approx 10^{-5}$ a.u.). The occupied excited states are energetically above the Fermi level of the metal and may resonantly decay into the empty conduction band. In this experiment, one needs an additional strong external electric field perpendicular to the surface to retract the ionized atom [9]. A step towards the theoretical analysis of such an experiment has been done recently by Nordlander and Dunning [8,10]. Within the fixed-atom approximation, they applied the complex-scaling method [11,12] to calculate energies and widths of atomic resonances formed under the combined influence of the surface potential and an external potential. Subsequently, using the calculated resonance parameters as input, they solved time-dependent classical rate equations to determine ion production rates as a function of the atom-surface distance. In the present work, first results of a *fully quantal*, time-dependent treatment of the electronic degrees of freedom of resonance ionization of highly excited hydrogen atoms interacting with a metal surface in the presence of an external electric field are presented. We employ a close-coupling approach [5,13–18], using atomic resonance states calculated in the fixed-atom approximation as basis states.

II. THEORY

We expand the solution $|\Psi(t)\rangle$ of the time-dependent one-electron Schrödinger equation

$$i|\dot{\Psi}(t)\rangle=[T+V_S+V_C^{>}(t)+Fz]|\Psi(t)\rangle \tag{2.1}$$

in terms of adiabatic resonance states $|\phi_j(D(t))\rangle$ [16–18], which depend parametrically on time t via the atom-surface distance $D(t)$:

$$|\Psi(\vec{r};t)\rangle=\sum_{j=1}^{N} c_j(t)|\phi_j(\vec{r};D(t))\rangle\exp\left[-i\int^t dt' E_j(D(t'))\right]. \tag{2.2}$$

In Eq. (2.1) T is the kinetic energy and V_S is the surface-jellium potential given by

$$V_S(z)=\begin{cases} -V_0, & z<z_0 \\ V_e^{(i)}(z)+V_C^{(i)}(z;D), & z\geqslant z_0, \end{cases} \tag{2.3}$$

where the z axis is directed perpendicular to the metal surface and z_0 is determined from the condition

*Present address: Department of Physics and Astronomy, University of Tennessee, Knoxville, TN 37996-1200.

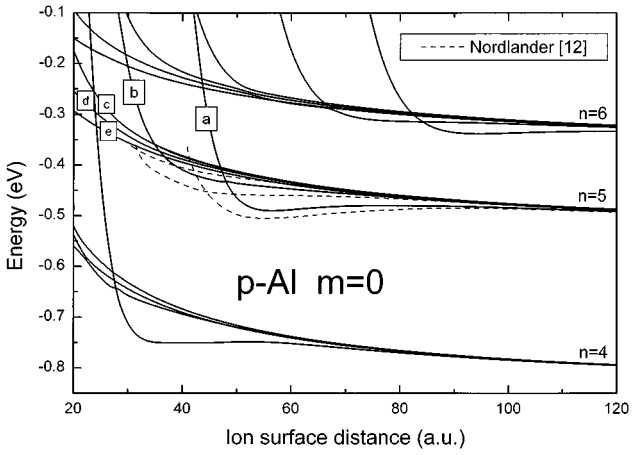

FIG. 1. Energies of the resonance states asymptotically converging to the $(n=4,5,6;\ m=0)$ manifolds for $F=0$. Labels a–e refer to the widths in Fig. 2. The dashed lines show results by Nordlander [12].

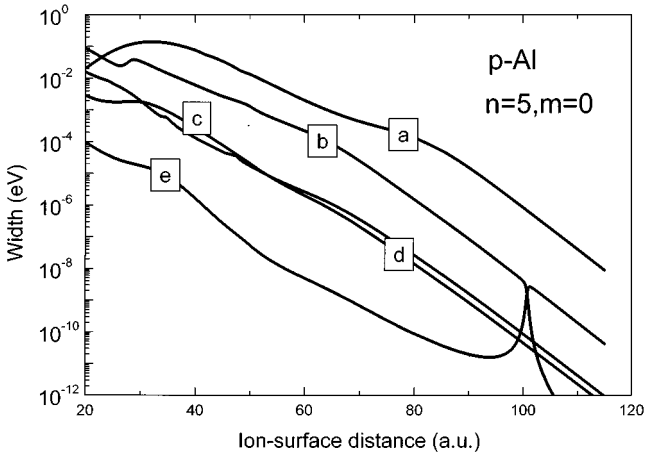

FIG. 2. Widths of the resonance states asymptotically converging to the $(n=5;\ m=0)$-manifold for $F=0$. Labels a–e refer to the energies in Fig. 1.

$$V_e^{(i)}(z_0)+V_C^{(i)}(z_0;D)=-V_0. \tag{2.4}$$

The potentials $V_e^{(i)}$ and $V_C^{(i)}(t)$ are the electronic self-image potential and the image potential induced by the core Coulomb potential $V_C^{>}(t)$ and are given by

$$V_e^{(i)}(z)=-\frac{1}{4z}\Theta(z) \tag{2.5}$$

and

$$V_C^{(i)}(\vec{r};D)=\frac{Z}{|\vec{r}+D\hat{e}_z|}\Theta(z)\approx\frac{Z}{|z+D|}\Theta(z). \tag{2.6}$$

The potential $V_C^{>}(t)$ is the Coulomb potential of the atomic core, fully screened inside the metal. The term Fz in Eq. (2.1) corresponds to a uniform electric field of strength F directed along the surface normal.

The evaluation of the resonance basis states $|\phi_j(D)\rangle$ is performed by solving the time-dependent Schrödinger equation (2.1) in a *fixed-atom* approximation using the self-energy method [5,15–18]. Basically, the self-energy method consists in (i) performing a two-center expansion of the total wave function in terms of *unperturbed* bound states of the atom and of the jellium metal and (ii) formally eliminating the explicit dependence on the wave functions of the jellium metal at the expense of introducing a complex *optical potential*. The resonance states $|\phi_j(D)\rangle$ are then obtained as eigenfunctions of the complex non-Hermitian self-energy matrix with complex eigenvalues $\omega_j=E_j-i\,\Gamma_j/2$ and are given as linear combinations of the *unperturbed* bound atomic states.

Inserting the expansion (2.2) into the time-dependent Schrödinger equation (2.1) leads to the set of close-coupling equations

$$\dot{c}_j(t)=-\sum_{j'=1}^{N} c_{j'}(t)\langle\phi_j(D(t))|\frac{\partial}{\partial t}+\frac{\Gamma_j}{2}\delta_{jj'}|\phi_{j'}(D(t))\rangle \times\exp\left[-i\int^t dt'(E_{j'}-E_j)\right]. \tag{2.7}$$

Overlap corrections between the resonance states have been neglected, i.e., $\langle\phi_j(D)|\phi_{j'}(D)\rangle=\delta_{jj'}$. Numerically, we found the largest overlap at small ion-surface distances to be less than 5%. The off-diagonal velocity-dependent couplings between the resonance states $|\phi_j(D)\rangle$ are caused by the operator $\partial/\partial t$, which, for perpendicular incidence at constant velocity v, can be rewritten as $-v\,\partial/\partial D$. The diagonal width term $\Gamma_j/2$ in Eq. (2.7) describes the decay of the resonance state $|\phi_j(D)\rangle$ into empty conduction-band states (we consider only resonance states that lie energetically above the Fermi level of the metal at all distances D). For a given initial population $\{c_j(t=-\infty)\}$ of the resonance states, the total probability $P_I(t)$ for ionization to occur until time t is

$$P_I(t)=1-\sum_{j=1}^{N}\ |c_j(t)|^2\ . \tag{2.8}$$

Classical rate equations similar to those used by Nordlander and Dunning [8] can be reproduced from our quantum approach by suppressing off-diagonal couplings in the close coupling equations.

III. RESULTS AND DISCUSSION

In this work we investigate the case of an excited hydrogen atom approaching an Al surface in normal incidence. Because of the cylindrical symmetry of the Hamiltonian, the m quantum number can be used to characterize the resonance states and different m manifolds do not couple. In our close-coupling calculation we included all hydrogenic states with $n\leqslant 6$ and $m=0$ and obtained convergence at all distances shown in this work for states asymptotically merging into the $n=5$ and lower manifolds. For the asymptotic $n=6$ manifold convergence is restricted to distances larger than about

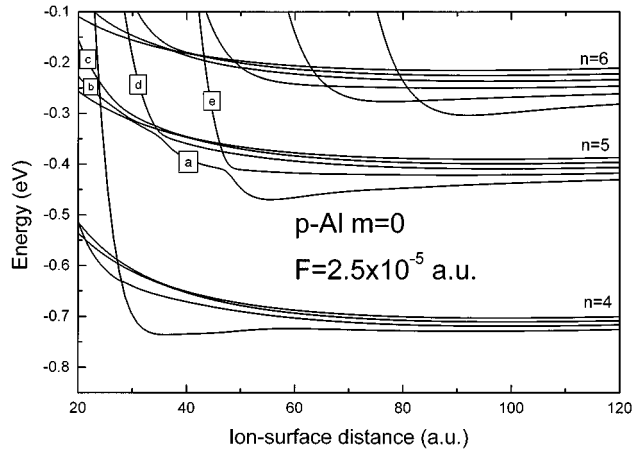

FIG. 3. Energies of the resonance states asymptotically converging to the $(n=4,5,6;\ m=0)$ manifolds for $F=2.5\times10^{-5}$ a.u. Labels a–e refer to the widths in Fig. 4.

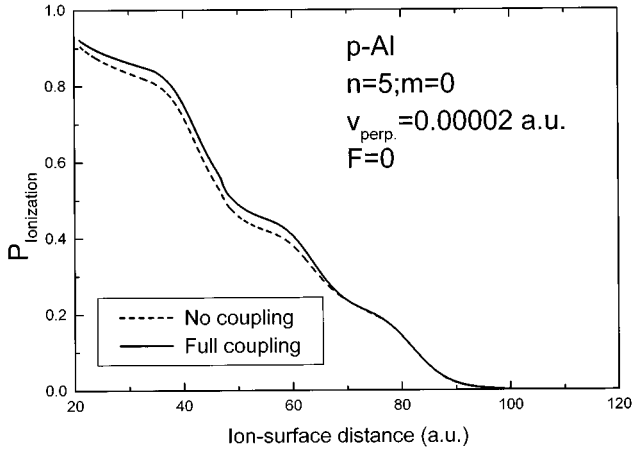

FIG. 5. Total ion production for $F=0$. The normal velocity is 2.0×10^{-5} a.u. Dashed line: no dynamic coupling. Full line: full dynamic coupling.

80 a.u. Figure 1 shows the energies of stationary resonance states versus the atom-surface distance for the asymptotic $(n=4,5,6;m=0)$- manifolds in the field-free case $(F=0)$. We diabatized energy and width diagrams (Figs. 1–4) by calculating the overlap matrix between all states of adjacent atom-surface distances and by connecting energies and widths with maximum overlap. In Fig. 1 we have also plotted the energy of resonance states as obtained by Nordlander who used the complex scaling method to solve the stationary Schrödinger equation for an ion interacting with a surface potential calculated by means of density functional theory [12]. Although this method yields a more accurate surface potential our results show the same overall behavior. The weaker binding energies at large atom-surface distances of our resonance states (as compared with energies of Ref. [12]) result from our approximation [15,18] of the classical nuclear image potential [see Eq. (2.6)] induced by the ion core, which slightly overestimates the nuclear image potential for all atom-surface distances.

Figure 2 reveals the widths of the resonance states to have a rather monotonic exponential shape. Exceptions to this rule can be seen at large atom-surface distances where a non-exponential behavior of the widths of two particular states can been seen. Similar non-exponential structures in the widths of resonance states have been reported by Nordlander [12] in the whole range of asymptotic $n=5$–18 manifolds. The nonexponential behavior appears at large D where both resonance states are nearly degenerate.

An additional external electric field leads to the Stark splitting of the asymptotic (n,m) manifolds. For the case of the $(n=4,5,6;\ m=0)$-manifolds Figs. 3 and 4 show the energies and widths of resonance states for a field strength of 2.5×10^{-5} a.u.$=1.3\times10^{5}$ V/cm. The chosen external electric field tends to preserve the overall structure of the level diagram and is small compared to the field strength needed for field ionization. As can be seen from both Fig. 2 and Fig. 4 the widths of resonance states span several orders of magnitude. If one assumes that the initial population of a hydrogenic (n,l,m) state leads to a statistical population of a specific (n,m) manifold due to the mixing through any weak electric field, one expects states with a large width to be

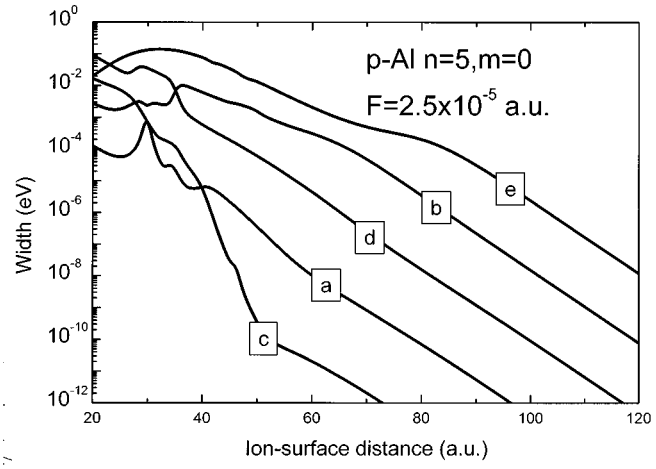

FIG. 4. Widths of the resonance states asymptotically converging to the $(n=5;m=0)$ manifold for $F=2.5\times10^{-5}$ a.u. Labels a–e refer to the widths in Fig. 3.

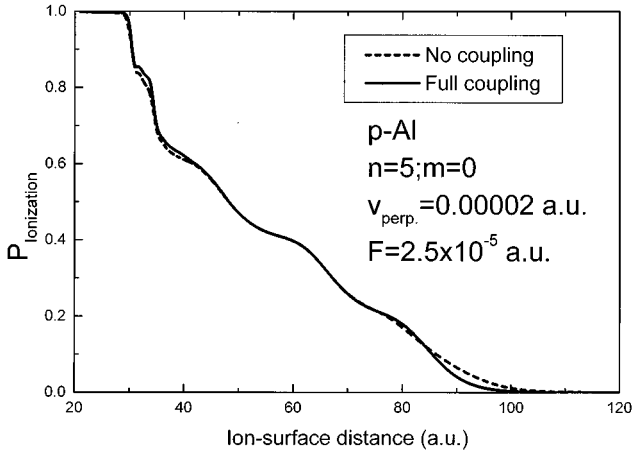

FIG. 6. Total ion production for $F=2.5\times10^{-5}$ a.u. The normal velocity is 2.0×10^{-5} a.u. Dashed line: no dynamic coupling. Full line: full dynamic coupling.

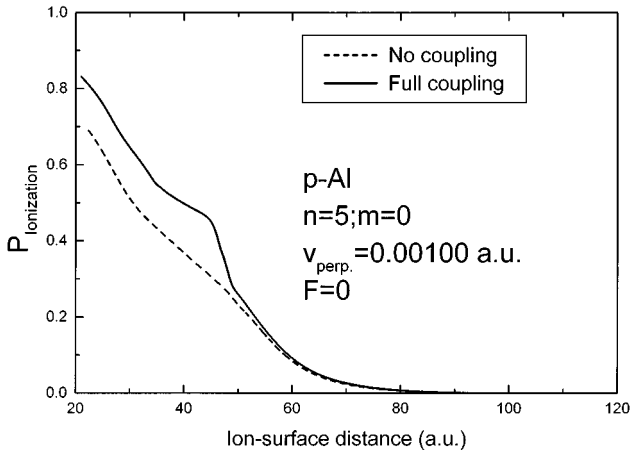

FIG. 7. Total ion production for $F=0$. The normal velocity is 1.0×10^{-3} a.u. Dashed line: no dynamic coupling. Full line: full dynamic coupling.

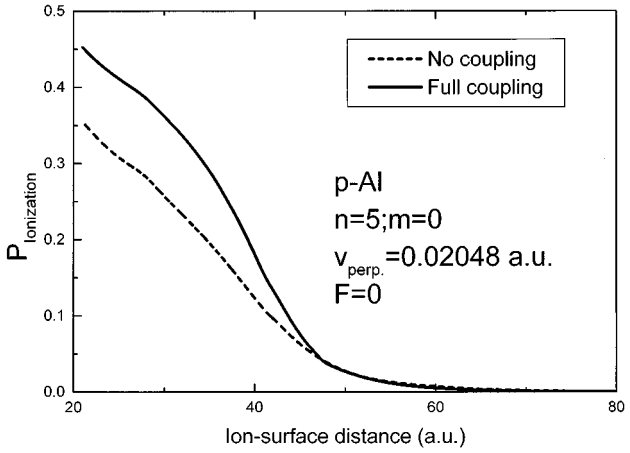

FIG. 9. Total ion production for $F=0$. The normal velocity is 2.048×10^{-2} a.u. Dashed line: no dynamic coupling. Full line: full dynamic coupling.

depopulated at far bigger atom-surface distances than those with a small width.

The aim of this paper is to investigate the velocity dependence of dynamic couplings between the adiabatic resonance states while the ion approaches the surface. We performed calculations for perpendicular velocities in the range of 2×10^{-5} to 2.048×10^{-2} a.u. both for the field free case and for the case of an ion moving in an external electric field of 2.5×10^{-5} a.u. perpendicular to the surface and directed so as to retract positive ions from the surface.

We solved Eq. (2.7) by considering an excited hydrogen atom with statistical population of the $(n=5;\ m=0)$ manifold while taking all $n=4$–6 adiabatic basis states into account. As a first test we studied probability transfer from the $n=5$ to the $n=4$ and $n=6$ manifolds in the range of velocities given above. It turned out that charge transfer between different n manifolds is negligible and convergence with respect to the size of the basis is therefore achieved.

In the region of subthermal velocities ($v=2\times10^{-5}$ a.u.) relevant for the proposed experiments [9] dynamic couplings indeed play a very minor role. This can be clearly seen in Fig. 5 showing $P_I(D(t))$ according to Eq. (2.7) for both full coupling among adiabatic states and no coupling while no external electric field was applied. For all ion-surface distances P_I is slightly larger for the case of full coupling. Figure 6 shows that the discrepancies between full coupling and no coupling results are further reduced if an additional external electric field of $F=2.5\times10^{-5}$ a.u. is applied. This is quite understandable as the external electric field leads to level splittings and thus efficiently reduces the effect of off-diagonal couplings. When raising the perpendicular velocity of the ion to the thermal velocity of 10^{-3} a.u., discrepancies in P_I occur between the full coupling and no coupling case for both the field-free ($F=0$) and $F=2.5\times10^{-5}$ a.u. case (Figs. 7 and 8). The discrepancy rises suddenly as the ion approaches the surface to about $D=50$ a.u. and is due to probability flux into the *large-width* resonance state denoted as a in Figs. 1 and 2 and as e in Figs. 3 and 4. Figures 9 and 10 show results for the ionization probability $P_I(D(t))$ where the perpendicular velocity of the incident atom has been further increased to 2.048×10^{-2} a.u. Although the interaction time is drastically reduced, dynamic couplings be-

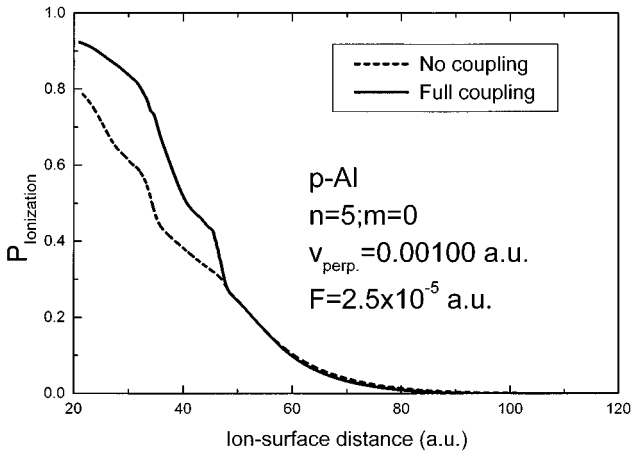

FIG. 8. Total ion production for $F=2.5\times10^{-5}$ a.u. The normal velocity is 1.0×10^{-3} a.u. Dashed line: no dynamic coupling. Full line: full dynamic coupling.

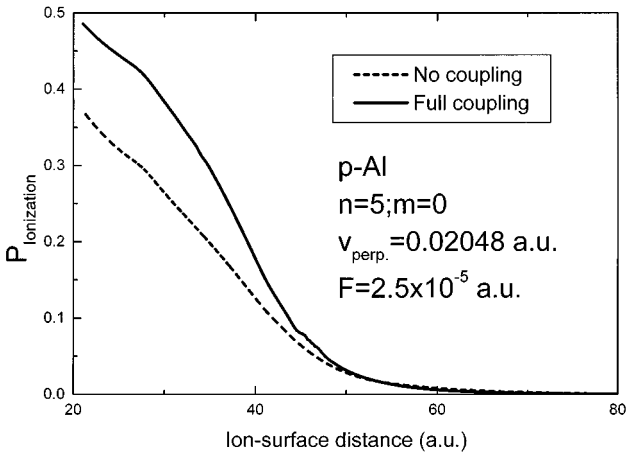

FIG. 10. Total ion production for $F=2.5\times10^{-5}$ a.u. The normal velocity is 2.048×10^{-2} a.u. Dashed line: no dynamic coupling. Full line: full dynamic coupling.

come significant and lead to a 10% higher ionization probability for the fully coupled case as compared to the rate-equation-like uncoupled case. Among the dynamical couplings acting between the five states of the ($n=5$; $m=0$) manifold several couplings can be identified as dominant: in the field-free case there is a strong interaction at $D=100$ a.u. among the states denoted as b and e in Fig. 1, which leads to a probability transfer towards the *large-width* state e. A second coupling acts among the resonance states denoted as b and c in Fig. 1. This is a long-range coupling, which slowly depopulates state b in favor of state c. For the case of an additional external electric field dominant couplings act among the states denoted as a and e at $D=45$ a.u., between a and d at $D=35$ a.u. and furthermore between b and c in the range of $D=20-45$ a.u. These dominant couplings lead to probability redistribution among the $n=5$ manifold and therefore to a different decay pattern as compared to the no-coupling case where each resonance state decays independently into the unoccupied states of the metal.

IV. CONCLUSION

In summary, we have presented close-coupling calculations for the ionization of highly excited hydrogen atoms interacting with an Al-metal surface both in the presence of a strong external electric field and for the field free case. The self-energy method used to generate both the resonance basis functions and complex energies allows one to perform the close-coupling calculations using a small set of basis functions. Our results for ion production in collisions of hydrogen with an Al surface show that quantum-mechanical dynamic couplings among resonance states play a minor role at subthermal velocities of the ion but lead to a significant rearrangment of the charge density for perpendicular velocities greater than 10^{-3} a.u. In general, dynamic couplings are more important for the field-free case due to the near-degeneracy of the resonance states.

ACKNOWLEDGMENTS

This work was supported by the Division of Chemical Sciences, Basic Energy Sciences, Office of Energy Research, U.S. Department of Energy, the Deutsche Forschungsgemeinschaft (DFG) through a postdoctoral grant for P.K., and the National Science Foundation through the Kansas Center for Advanced Scientific Computing.

[1] C. Fabre, M. Gross, J. M. Raimond, and S. Haroche, J. Phys. B **16**, L671 (1983).
[2] G. E. McCown, C. R. Taylor, and C. A. Kocher, Phys. Rev. A **38**, 3918 (1988).
[3] D. F. Gray, Z. Zheng, K. A. Smith, and F. B. Dunning, Phys. Rev. A **38**, 1601 (1988).
[4] C. A. Kocher and G. E. McCown, Surf. Sci. **244**, 321 (1991).
[5] J. Burgdörfer, in *Review of Fundamental Processes and Applications of Atoms and Ions*, edited by C. D. Lin (World Scientific, Singapore, 1993), p. 517.
[6] H. Winter, J. Phys.: Condens. Matter **8**, 10 149 (1996).
[7] H. D. Hagstrum, in *Electron and Ion Spectroscopy of Solids*, edited by L. Fiermans, J. Vennik, and W. Dekeyser (Plenum, New York, 1978), p. 273.
[8] P. Nordlander and F. B. Dunning, Phys. Rev. B **53**, 8083 (1996).
[9] P. Nordlander and F. B. Dunning (private communication).
[10] P. Nordlander and F. B. Dunning, Nucl. Instrum. Methods Phys. Res. B **125**, 300 (1997).
[11] P. Nordlander and J. C. Tully, Phys. Rev. B **42**, 5564 (1990).
[12] P. Nordlander, Phys. Rev. B **53**, 4125 (1996).
[13] J. C. Tully, Phys. Rev. B **16**, 4324 (1977).
[14] O. Plotzke, U. Wille, R. Hippler, and H. O. Lutz, Phys. Rev. Lett. **65**, 2982 (1990).
[15] P. Kürpick, U. Thumm, and U. Wille, Nucl. Instrum. Methods Phys. Res. B **125**, 273 (1997).
[16] J. Burgdörfer, E. Kupfer, and H. Gabriel, Phys. Rev. A **35**, 4963 (1987).
[17] P. Kürpick and U. Thumm, Phys. Rev. A **54**, 1487 (1996).
[18] P. Kürpick, U. Thumm, and U. Wille, Phys. Rev. A **56**, 543 (1997).